HHS Public Access

Author manuscript

Mol Imaging Biol. Author manuscript; available in PMC 2021 June 01.

Published in final edited form as:

Mol Imaging Biol. 2020 June ; 22(3): 722–729. doi:10.1007/s11307-019-01409-3.

Ferumoxytol does not impact Standardized Uptake Values on PET/MR scans

Anne M. Muehe, MD[1], **Ketan Yerneni, BA**[1], **Ashok J. Theruvath, MD**[1], **Avnesh S. Thakor, MD, PhD**[1], **Alison Pribnow, MD**[2], **Raffi Avedian, MD**[3], **Robert Steffner, MD**[3], **Jarrett Rosenberg, PhD**[1], **Kristina E. Hawk, MD, PhD**[1], **Heike E. Daldrup-Link, MD, PhD**[1,2]

[1]Department of Radiology, Pediatric Molecular Imaging Program, Stanford University

[2]Department of Pediatrics, Pediatric Hematology/Oncology, Lucile Packard Children's Hospital

[3]Department of Orthopedic Surgery, Lucile Packard Children's Hospital, Stanford University

Abstract

Purpose: Tumor response assessments on positron emission tomography (PET)/magnetic resonance imaging (MRI) scans requires correct quantification of radiotracer uptake in tumors and normal organs. Historically, MRI scans have been enhanced with gadolinium (Gd) based contrast agents, which are now controversial due to brain deposition. Recently, ferumoxytol nanoparticles have been identified as an alternative to Gd-based contrast agents, because they provide strong tissue enhancement on MR images but are not deposited in the brain. However, it is not known if the strong T1- and T2-contrast obtained with iron oxide nanoparticles such as ferumoxytol could affect MR-based attenuation correction of PET data. The purpose of our study was to investigate, if a ferumoxytol administration prior to a 2-deoxy-2-[^{18}F]fluoro-D-glucose [^{18}F]FDG PET/MR scan would change standardized uptake values (SUV) of normal organs.

Procedures: 30 pediatric patients (6-18 years) with malignant tumors underwent [^{18}F]FDG-PET/MR scans (dose 3 MBq/kg). Fifteen patients received an intravenous ferumoxytol injection (5 mg Fe/kg) prior to the [^{18}F]FDG-PET/MR scans (group 1). 15 additional age- and sex-matched patients received unenhanced [^{18}F]FDG-PET/MR scans (group 2). For attenuation correction of PET data, we used a Dixon-based gradient echo sequence (TR 4.2 ms, TE 1. 1, 2.3 ms, FA 5), which accounted for soft tissue, lung, fat and background air. We used a mixed linear effects model to compare the tissue MRI enhancement, quantified as the signal-to-noise ratio (SNR), as well as tissue radiotracer signal, quantified as SUVmean and SUVmax, between group1 and group 2. Alpha was assumed at 0.05.

Corresponding author: Heike E. Daldrup-Link, Molecular Imaging Program at Stanford, Stanford University, 725 Welch Road, Stanford, CA 94304, phone: (650) 723-8996; fax: (650) 725-8957; heiked@stanford.edu.

Conflict of interest: The authors declare that they have no conflict of interest.

Ethical Approval: All procedures performed in studies involving human participants were in accordance with the ethical standards of the institutional and national research committees and with the 1964 Helsinki declaration and its later amendments or comparable ethical standards.

Informed Consent: Informed consent was obtained from all individual participants included in the study.

Results: The MRI enhancement of the blood and solid extra-cerebral organs, quantified as SNR, was significantly higher on ferumoxytol-enhanced MRI scans compared to unenhanced scans ($p < 0.001$). However, SUVmean and SUVmax values, corrected based on the patients body weight or body surface area, were not significantly different between the two groups ($p > 0.05$).

Conclusion: Ferumoxytol administration prior to a [^{18}F]FDG PET/MR scan did not change standardized uptake values (SUV) of solid extra-cerebral organs. This is important, because it allows to inject ferumoxytol contrast prior to a PET/MRI procedure and thereby, significantly accelterate image acquisition times.

Keywords

PET/MR Imaging; Iron Oxide Nanoparticles; Cancer Imaging; Pediatric Cancer; Standardized Uptake Values

Introduction

Tumor response assessments on positron emission tomography (PET)/magnetic resonance imaging (MRI) scans requires correct quantification of radiotracer uptake in tumors and normal organs. SUV measurements can help estimate tumor grade and predict clinical outcomes [1-2]. PET imaging requires the detection of annihilated photons, which travel from different depths of the body to the PET detectors. An attenuation correction (AC) algorithm is necessary to account for differences in attenuation for photons originating at different locations. Magnetic resonance (MR) imaging cannot directly calculate the radiodensity of tissues. The most widely used method for MR-based AC is based on tissue segmentation with an in- and out-of- phase gradient echo (GRE) sequence, which creates water-only images and fat-only images, which can define four different tissue classes (air, lung, fat, soft tissue) [3-4]. However, GRE sequences are susceptible to artifacts which can lead to misclassification of tissue and underestimation of SUV. A recent study showed that AC-maps after Gadolinium (Gd) administration lead to tissue misclassifications in 40% of patients [5].

Ferumoxytol is an iron oxide nanoparticle compound that can be used “off label” as a contrast agent for integrated PET/MR scans, and has several advantages over Gd-chelates including long lasting vessel contrast and tissue enhancement [6]. In addition, ferumoxytol accumulates in the reticuloendothelial system and improves the detection of metastases in liver, spleen, bone marrow and lymph nodes [7-8]. It is not known whether ferumoxytol administration will impair attenuation correction of 2-Deoxy-2-[^{18}F]fluoroglucose ([^{18}F]FDG)-PET data on integrated PET/MR scans. Borra et al. recently described that high doses of ferumoxytol (10 mg Fe/kg) affected MR-based attenuation correction of PET data in a monkey [9]. The high doses of ferumoxytol caused at T2 effect (dark MRI signal) of the liver on a T1-weighted Dixon sequence; therefore, liver tissue which accumulated ferumoxytol was mistakenly classified as lung tissue. This led to miscalculation of SUVs in the monkey and could affect the assessment of treatment response in a patient. However, the ferumoxytol dose applied for clinical scans is much lower, in the order of 3-5 mg Fe/kg and causes a positive (bright) signal enhancement on T1-weighted MR images [10-12].

Therefore, the soft tissue classification of liver tissue does not change before and after ferumoxytol.

Here, the purpose of our study was to evaluate if SUV generated from ferumoxytol-enhanced or unenhanced MRAC maps were significantly different. We hypothesized that SUV of normal organs would not be significantly different on [^{18}F]FDG-PET scans, if these were corrected with ferumoxytol-enhanced or unenhanced AC-maps.

Materials and Methods:

For this HIPAA compliant and institutional review board (IRB) approved study, we selected [^{18}F]FDG-PET/MR images from an ongoing prospective single center clinical trial (NCT01542879 for ferumoxytol-enhanced scans) and a pediatric PET/MR image registry (NCT03458520 for unenhanced scans) for the case controls. An informed consent form was signed from adult subjects or parents and assent was obtained from minors.

Group 1 (ferumoxytol): Inclusion criteria for ferumoxytol-enhanced scans comprised of the following: (1) age 6-18 years, (2) extracranial malignancy and (3) [^{18}F]FDG-PET/MR scan. Exclusion criteria were (1) MR-incompatible metal implants, (2) claustrophobia, (3) hemosiderosis/ hemochromatosis and (4) history of allergies to iron products or any history of severe anaphylactic reactions. These patients comprised 8 males and 7 females with a mean age of 13.1 years (range 8-18 years), with 7 sarcomas, 3 lymphomas, and 5 other tumors.

Group 2 (no ferumoxytol): Each patient who received a ferumoxytol-enhanced scan was retrospectively age and sex-matched with a patient who underwent a PET/MR scan without contrast agent. These scans were matched in time to account for potential software fluctuations and variation in MR tuning and PET calibrations. These 15 patients who underwent unenhanced scans comprised 8 males and 7 females with a mean age of 12.4 years (range 6-18 years), with 5 lymphomas, 4 sarcomas, and 6 other tumors.

We performed a power analysis, which indicated that 15 patients per group provides a strong enough sample size to determine the overall effect. Detailed demographics of all patients are shown in Suppl. Table 1 (see Electronic Supplementary Material (ESM)). None of the scans was performed under general anesthesia or sedation.

Imaging

Patients in group 1 underwent whole-body [^{18}F]FDG-PET/MR imaging at 1-24 h after infusion of ferumoxytol (dose 5 mg Fe/kg) and at 50 min (± 14 min) after intravenous [^{18}F]FDG injection (dose 3 MBq/kg, mean: 148.1 ± 55 MBq). Ferumoxytol was administered with investigational new drug (IND) approval (IND 111 154) from the food and drug administration for off-label use of the iron supplement ferumoxytol (Feraheme®, AMAG Pharmaceuticals, Inc., Waltham, MA) as an MR contrast agent. Ferumoxytol nanoparticles consist of a magnetite and maghemite core and a carboxymethyldextran coating. The mean hydrodynamic diameter of the nanoparticles is 30 nm, which leads to a long blood half-life of approximately 19 h in patients. For doses relevant to this project,

ferumoxytol nanoparticles generally cause hyperintense (bright) tissue MRI signal on T1-weighted MR images and hypointense (dark) MRI signal on T2-weighted MR images (with some exceptions). Patients in group 2 underwent unenhanced [^{18}F]FDG-PET/MR scans at 50 min (± 18 min) after intravenous injection of [^{18}F]FDG at a dose of 3 MBq/kg (mean: 179.2 ± 82 MBq). We position children in the PET/MRI scanner slightly earlier than in a PET/CT scanner in order to adjust for the time need to place whole body MRI coils and prescribe the PET/MRI protocol. This leads to a start of the scan at 60 minutes after FDG injection, which is equivalent to a PET/CT scan.

All [^{18}F]FDG-PET/MR scans were obtained on an integrated 3T PET/MR scanner (Signa, GE Healthcare, Chicago, IL), using a 32-channel torso phased array coil and an eight-channel, receive-only head coil. Pulse sequences comprised axial T1-weighted two-point Dixon Liver Acquisition with Volume Acquisition (LAVA) sequences (3D Fast Spoiled Gradient Echo repetition time (TR) 4.2 ms, echo time (TE) 1.1, 2.3 ms, flip angle (FA) 5) for attenuation correction, and a higher resolution LAVA sequence (TR 4.4 ms, TE 1.1, 2.2 ms, FA 15) for anatomical co-registration. All sequences were obtained with a slice thickness of 3 mm, a FOV of 38 cm, a bandwidth of 142 kHz, and a matrix of 320 × 224 pixels. PET data were acquired simultaneously with a 25 cm axial FOV and 4 min acquisition per slab. We generated 4-tissue-class (long, soft tissue, fat and background/air) attenuation maps from the MR data acquired using the T1-weighted Dixon sequence as previously reported [3-4].

Data analysis

MR—We measured the signal intensity of the mediastinal blood pool, brain, parotid gland, thymus, myocardium, liver, spleen, bone marrow, adrenal gland, kidney, and gluteus maximus muscle on ferumoxytol and unenhanced MRAC-LAVA scans with OSIRIX Software (Osirix, Bernex, Switzerland) by placing a region of interest (ROI; diameter: 1 cm) over the organ of interest, in symmetric organs in the left side, carefully avoiding vessels. For the adrenal gland we adjusted the size of the ROI to fit the organ. In addition, we measured the background signal in phase encoding direction above or below the organ of interest. We calculated the signal to noise ratio (SNR) as

$$SNR = \frac{mean\ signal\ intensity\ (organ)}{standard\ deviation\ of\ background\ signal}$$

PET—We reconstructed the [^{18}F]FDG-PET data using a 3D time of flight iterative ordered subsets expectation maximization algorithm (24 subsets, 3 iterations, temporal resolution=400 ps, matrix 192 × 192; voxel size 2.8×2.8×2.8 mm, Gaussian filter 4 mm) and MR attenuation correction using the resultant data with the manufacturer provided method [4]. We imported reconstructed and attenuation corrected [^{18}F]FDG-PET and MR data to MIM 6.5 (MIM Software, Inc, Cleveland, OH).

To assess the effect of ferumoxytol on SUVmean and SUVmaximum values of the mediastinal blood pool and normal organs, we placed three dimensional ROIs (diameter: 1 cm) over specified regions of the brain, parotid gland, larynx (adjusted ROI to organ size), thymus, myocardium, liver (3 cm), spleen (2 cm), bone marrow, kidney, and gluteus maximus muscle. We calculated the SUVmean and SUVmaximum based on the bodyweight

(SUV bw). Likewise, when accounting for the body surface area (bsa), the $SUVmean_{bsa}$ of the mediastinal blood pool were calculated; subsequently, the SUVmax of the brain and nine different organs were normalized to it. The SUV_{bsa} is less dependent on body habitus than the SUV_{bw}, especially in patients with increased portion of body fat [13-14].

$$\text{SUVbw} = \frac{tissue\ tracer\ activity\ (mCi\ /\ g)}{(injected\ dose (mCi)\ /\ patient\ body\ weight\ (kg))}$$

$$\text{SUVbsa} = \frac{tissue\ tracer\ activity\ (mCi\ /\ g)}{(injected\ dose\ (mCi)\ /\ patient\ body\ surface\ area\ (m^2))}$$

To evaluate whether ferumoxytol administration causes tissue misclassifications on AC-maps, two observers evaluated ferumoxytol-enhanced and unenhanced AC-maps. The observers were blinded to the study group (group 1 or 2) and evaluated AC-maps on images with a preset window level (950) and window width (250).

Statistical Analyses

The mean signal to noise ratio of different organs measured on ferumoxytol-enhanced and unenhanced MRAC were compared. The effect of ferumoxytol-enhanced versus unenhanced MRAC on mean signal to noise ratio – as well as maximum and mean SUV of brain and 9 different organs – were predicted based upon a mixed-effects model with the organ as a covariate.

SUVmean and SUVmaximum of organs were normalized to SUVmean and SUVmaximum of the mediastinal blood pool as it is used as an internal standard within either the bw or bsa group [13-14]. Kolmogrov-Smirnov (KS) tests were conducted and quantile-quantile (QQ) plots were produced to show the equality of two (ferumoxytol and no ferumoxytol group) distributions for SUV. Sample size was determined primarily by availability. A power analysis indicated that sample sizes of 15 in each group would provide 98% power at a 5% error to detect an effect size of 1.5 standard deviations, and 78% power to detect an effect size of one standard deviation. All statistical analyses were done with Stata Release 15.1 (StataCorp LP, College Station, TX), using a significance level of 0.05.

Results

Ferumoxytol caused significant positive tissue and vascular enhancement on T1-weighted LAVA images (Fig 1). SNR values of the mediastinal blood pool, brain, and normal organs were significantly increased on ferumoxytol-enhanced LAVA images (group 1) compared to unenhanced images (group 2; $p < 0.001$; Fig. 2). However, the AC-maps and [^{18}F]FDG-PET scans in group 1 and 2 showed no visually discernible differences (Fig. 3).

Next, SUV were normalized to mediastinal blood pool as it is used as an internal standard. For raw values of each subject see Suppl. Table 2 (see ESM). The SUVmax values of the brain and nine different visceral organs, calculated based on the patient's body weight (bw), showed no significant difference on ferumoxytol-enhanced and unenhanced AC-corrected

[^{18}F]FDG-PET scans (all p>0.05, Fig. 4a). The SUVmean$_{bw}$ of the brain and nine different visceral organs showed no significant difference on ferumoxytol-enhanced and unenhanced AC-corrected PET scans (all p > 0.05, Fig. 4b).

Likewise, when accounting for the body surface area (bsa), the SUVmean$_{bsa}$ values of the mediastinal blood pool were calculated; subsequently, the SUVmax values of the brain and nine different visceral organs were normalized to it. SUVmax$_{bsa}$ showed no significant difference on ferumoxytol-enhanced and unenhanced AC-corrected PET scans (all p > 0.05, Suppl. Fig 1a, see ESM). SUVmean$_{bsa}$ values were also not significantly different on ferumoxytol-enhanced and unenhanced AC-corrected PET scans (all p > 0.05, Suppl. Fig. 1b, see ESM).

In addition, as we did not perform unenhanced [^{18}F]FDG-PET/MR scans on the same patients who received ferumoxytol due to feasibility issue, we conducted the KS test to show the equality of the two (ferumoxytol and non ferumoxytol) distributions (SUVmax$_{bw}$ p = 0.52; SUVmean$_{bw}$ p = 0.43; SUVmax$_{bsa}$ p = 0.97; SUVmean$_{bsa}$ p = 0.91) and produced QQ plots (Fig. 5).

Evaluation of AC-maps confirmed that all visceral organs and the brain on ferumoxytol-enhanced MRAC scans were correctly classified as soft tissue for the AC-maps (Fig. 3). We did not observe any new artifacts or misclassifications in the ferumoxytol group compared to the control group.

Discussion

Our data showed that ferumoxytol administration does not appear to affect SUV measurements on [^{18}F]FDG-PET/MR scans. Therefore, we conclude that it is not needed to obtain unenhanced Dixon sequences for attenuation correction before acquiring ferumoxytol-enhanced scans. This is important because acquisition of both unenhanced and contrast-enhanced scans would substantially prolong image data acquisition times [15].

This study systematically investigates the effect of ferumoxytol on quantitative PET imaging data assessments in humans. Borra et al. previously investigated the effect of ferumoxytol in phantoms and in liver, spleen, and pancreas of one single monkey [9]. In a single male baboon, intravenous injection of ferumoxytol at a dose of 10 mg Fe/kg caused decreased liver SUVmean value on contrast-enhanced compared to unenhanced scans. The corresponding AC-map showed that the signal of liver was falsely classified as air in this monkey. Conversely, we found no difference in SUV data for blood, liver or eight different visceral organs on ferumoxytol-enhanced and unenhanced PET/MR scans of 15 patients per group. This different result might be explained by the lower ferumoxytol dose of 5 mg Fe/kg in our study. Our T1-weighted LAVA scans showed a positive liver contrast enhancement, which was correctly classified as soft tissue.

Ferumoxytol causes a positive (bright) signal enhancement on T1-weighted MR AC sequences. Our dose was not so high that it caused a T2-signal effect on T1-weighted AC scans, in which a high dose of ferumoxytol can cause a T2 effect (hypointense artifact) on T1-weighted AC scans, which could have caused misregistration of soft tissue as air. In

accordance with our data, Borra et al. showed that ferumoxytol concentrations of 4 mg Fe/ml did not interfere with MR based attenuation correction of PET data in either liquid or chelated ferumoxytol probes in test tubes in a phantom [9].

We found no significant difference regarding tissue misclassification on AC-maps with or without ferumoxytol. Since AC sequences are typically T1-weighted, tissue misclassifications as bone or air would require very high iron doses and tissue concentrations to reach a T2 signal effect on T1-weighted images. Other investigators reported that the stomach in a single volunteer was misclassified as “lung” after oral administration of the iron based contrast agent ferumoxil with a standard Dixon-based AC correction sequence [16]. In our study, much lower iron concentrations in the blood pool and visceral organs caused a positive (bright) signal enhancement on T1-weighted scans, which was within the range of soft tissue. In accordance with our results, Lois et al. did not find any differences in SUVmean or SUVmax on unenhanced and gadolinium-enhanced PET/MR scans in one single patient [16].

One limitation of our study is that we did not perform unenhanced [^{18}F]FDG-PET/MR scans on the same patients who received ferumoxytol, because obtaining two [^{18}F]FDG-PET/MR scans was not feasible for our pediatric cancer patients due to the resulting increase in scan time as well as the additional radiation dose. Instead, we matched ferumoxytol patients with unenhanced controls by age-and sex and showed the distribution of SUV of both groups are the same. Furthermore, we used the standard vendor two-point Dixon sequence for attenuation correction instead of a UTE sequence, which would be more robust to potential susceptibility effects from iron. However, our study showed that attenuation correction is feasible, robust, and reliable with the two-point Dixon sequence when using ferumoxytol at a dose of 5 mg Fe/kg. The FDA-approved ferumoxytol dose for iron supplementation is 1020 mg (two doses of 510 mg with a 3-8 day interval), which is about four times higher than the dose used for MR imaging (5 mg Fe/kg = 250 mg Fe total in a 50 kg teenager). This is comparable to the iron dose delivered with one blood transfusion. While none of patients had any clinical signs of iron overload, ferumoxytol would be contraindicated in patients with hemosiderosis or hemochromatosis.

Conclusion

In conclusion, we demonstrate that a ferumoxytol dose of 5 mg Fe/kg does not appear to affect the attenuation correction in [^{18}F]FDG-PET/MR imaging. Using ferumoxytol instead of gadolinium chelates may solve problems related to concerns about gadolinium deposition in the brain, short-lasting vessel contrast and decreased image quality due to non-simultaneous image acquisition of [^{18}F]FDG-PET and MR images.

Supplementary Material

Refer to Web version on PubMed Central for supplementary material.

Acknowledgements:

We thank Dawn Holley and Harsh Gandhi from the PET/MR Metabolic Service Center for their assistance with the acquisition of PET/MR scans at the Lucas Research Center at Stanford. We thank Derrick Gillan and Aaron Wetzel for their assistance with the acquisition of PET/MR images at Lucile Packard Children's Hospital and for assistance with data transfer. We thank the members of Daldrup-Link lab for valuable input and discussions regarding this project. We thank Tie Liang for help with the statistical analysis.

Funding: This work was supported by a grant from the Eunice Kennedy Shriver National Institute of Child Health and Human Development, grant number R01 HD081123-01A1.

References

1. Davis JC, Daw NC, Navid F, et al. (2018) ^{18}F-FDG Uptake During Early Adjuvant Chemotherapy Predicts Histologic Response in Pediatric and Young Adult Patients with Osteosarcoma. J Nucl Med 59:25–30. [PubMed: 28611244]
2. Sandlund JT, Guillerman RP, Perkins SL, et al. (2015) International Pediatric Non-Hodgkin Lymphoma Response Criteria. J Clin Oncol 33:2106–2111. [PubMed: 25940725]
3. Wollenweber SD, Ambwani S, Lonn AHR, et al. (2013) Comparison of 4-Class and Continuous Fat/Water Methods for Whole-Body, MR-Based PET Attenuation Correction. IEEE Trans Nucl Sci 60:3391–3398.
4. Martinez-Moller A, Souvatzoglou M, Delso G, et al. (2009) Tissue classification as a potential approach for attenuation correction in whole-body PET/MRI: evaluation with PET/CT data. J Nucl Med 50:520–526. [PubMed: 19289430]
5. Ruhlmann V, Heusch P, Kuhl H, et al. (2016) Potential influence of Gadolinium contrast on image segmentation in MR-based attenuation correction with Dixon sequences in whole-body ^{18}F-FDG PET/MR. Magn Resonan Mater Phys Biol Med. 29:301–308.
6. Aghighi M, Theruvath AJ, Pareek A, et al. (2018) Magnetic Resonance Imaging of Tumor Associated Macrophages: Clinical Translation. Clin Cancer Res: DOI: 10.1158/1078-0432.CCR-18-0673.
7. Klenk C, Gawande R, Uslu L, et al. (2014) Ionising radiation-free whole-body MRI versus ^{18}F-fluorodeoxyglucose PET/CT scans for children and young adults with cancer: a prospective, non-randomised, single-centre study. Lancet Oncol 15:275–285. [PubMed: 24559803]
8. Lu M, Cohen MH, Rieves D, Pazdur R (2010) FDA report: Ferumoxytol for intravenous iron therapy in adult patients with chronic kidney disease. Am J Hematol 85:315–319. [PubMed: 20201089]
9. Borra RJ, Cho HS, Bowen SL, et al. (2015) Effects of ferumoxytol on quantitative PET measurements in simultaneous PET/MR whole-body imaging: a pilot study in a baboon model. EJNMMI Phys 2: doi.org/10.1186/s40658-015-0109-0.
10. Muehe AM, Theruvath AJ, Lai L, et al. (2018) How to Provide Gadolinium-Free PET/MR Cancer Staging of Children and Young Adults in Less than 1 h: the Stanford Approach. Mol Imaging Biol 20:324–335. [PubMed: 28721605]
11. Varallyay CG, Nesbit E, Fu R, et al. (2013) High-resolution steady-state cerebral blood volume maps in patients with central nervous system neoplasms using ferumoxytol, a superparamagnetic iron oxide nanoparticle. J Cereb Blood Flow Metab 33:780–786. [PubMed: 23486297]
12. Ning P, Zucker EJ, Wong P, Vasanawala SS (2016) Hemodynamic safety and efficacy of ferumoxytol as an intravenous contrast agents in pediatric patients and young adults. Magn Reson Imaging 34:152–158. [PubMed: 26518061]
13. Wahl RL, Jacene H, Kasamon Y, Lodge MA (2009) From RECIST to PERCIST: Evolving Considerations for PET response criteria in solid tumors. J Nucl Med 50 Suppl 1:122S–150S. [PubMed: 19403881]
14. Zasadny KR, Wahl RL (1993) Standardized uptake values of normal tissues at PET with 2-[fluorine-18]-fluoro-2-deoxy-D-glucose: variations with body weight and a method for correction. Radiology 189:847–850. [PubMed: 8234714]

15. Harisinghani M, Ross RW, Guimaraes AR, Weissleder R (2007) Utility of a new bolus-injectable nanoparticle for clinical cancer staging. Neoplasia 9:1160–1165. [PubMed: 18084623]

16. Lois C, Bezrukov I, Schmidt H, et al. (2012) Effect of MR contrast agents on quantitative accuracy of PET in combined whole-body PET/MR imaging. Eur J Nucl Med Mol Imaging 39:1756–1766. [PubMed: 22890801]

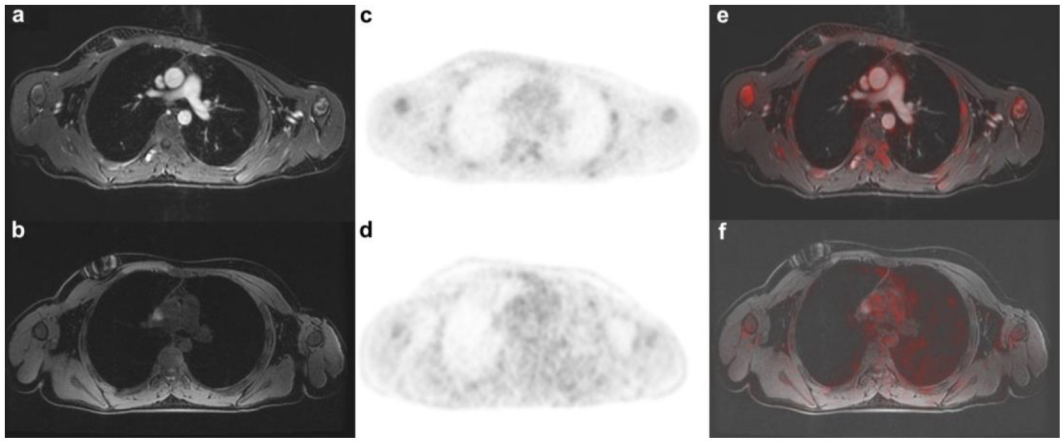

Figure 1.

Ferumoxytol-enhanced versus non-enhanced PET/MR: Images of age (15 years) and sex-matched (male) patients with rhabdomyosarcoma. Axial T1-weighted liver acquisition volume acquisition (LAVA, TR 4.4 ms/ TE 1.7 ms/ Flip angle 15) sections through the thorax delineate the vessels much better on **a** ferumoxytol enhanced than on **b** unenhanced images. On the corresponding MR-attenuation corrected (MAC) PET for **c** enhanced and **d** unenhanced scans the attenuation correction for mediastinal blood pool shows no difference. The fused PET/MR scans allow again better anatomical orientation and delineation of vessels on the **e** ferumoxytol- enhanced scans than on the **f** unenhanced scan.

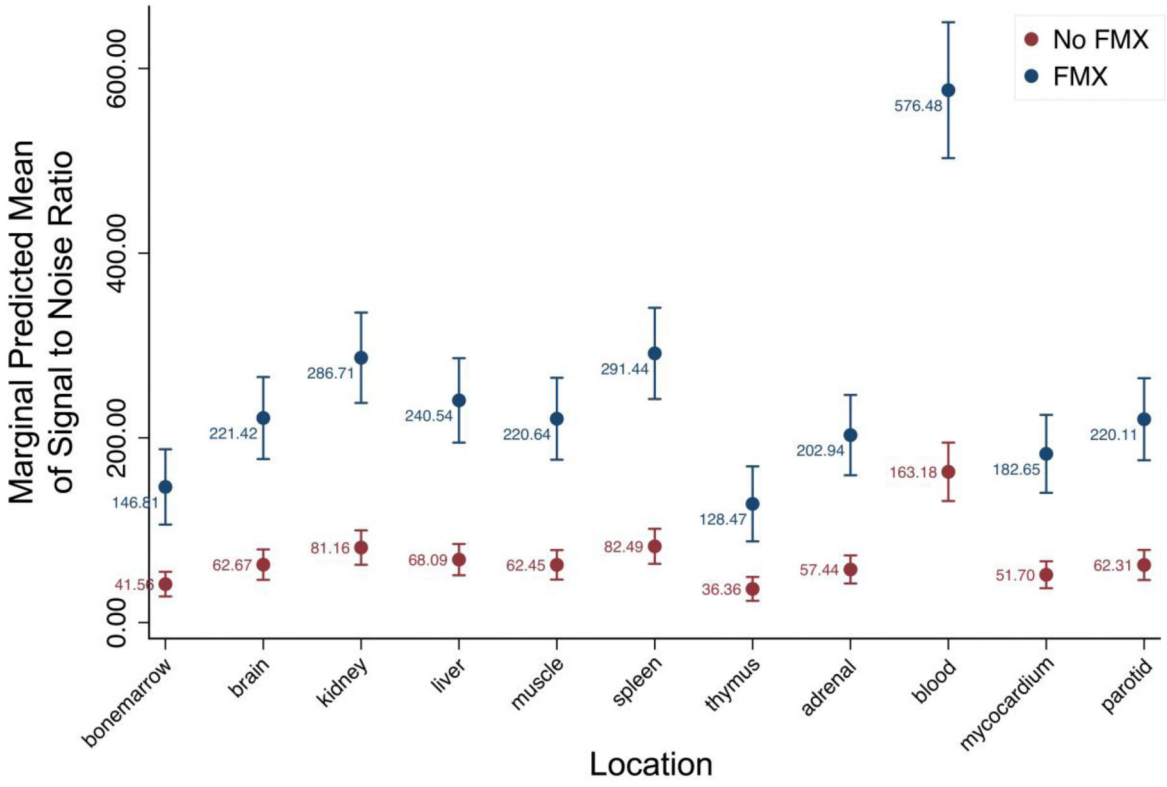

Figure 2.

Signal to noise ratio (SNR) of different organs, measured on ferumoxytol-enhanced and unenhanced MR images for attenuation correction (MRAC). All evaluated organs showed a significantly higher SNR on ferumoxytol-enhanced MRAC images (blue circles) compared to unenhanced MRAC (red circles) (* = $p < 0.001$).

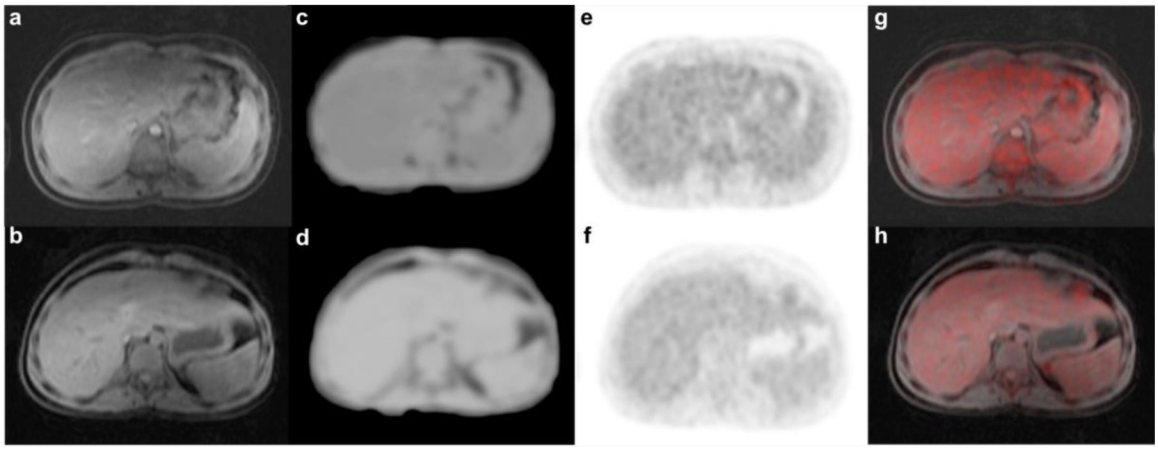

Figure 3.

Attenuation Correction map for ferumoxytol and unenhanced PET/MR scans. The MR sequence for attenuation correction (MRAC) (TR 4.1 ms/ TE 1.7 ms/ FA 5) on **a** ferumoxytol-enhanced and **b** unenhanced scans did not show tissue misclassification for liver in any of our patients. Attenuation correction maps correctly accounted liver as soft tissue in **c** enhanced as well as **d** unenhanced scans. PET was correctly attenuation-corrected on **e** enhanced as well as **f** unenhanced scans. Fusion of PET with **g** enhanced as well as **b** unenhanced MR again shows correct attenuation on both scans.

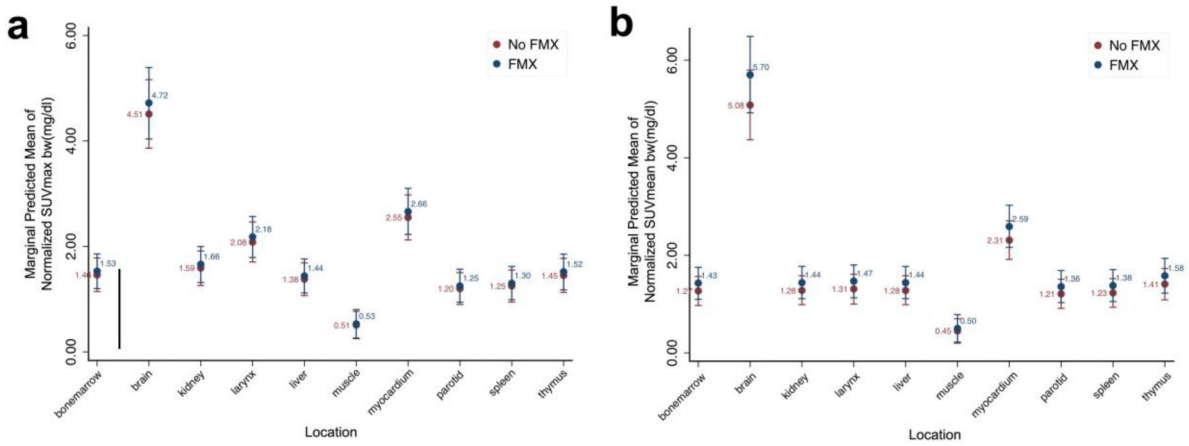

Figure 4.

Maximum standardized uptake values **a** SUVmax and **b** mean SUV of brain and 9 different organs, calculated as tissue tracer activity (mCi/g) divided by injected dose (mCi) through patient body weight (bw). No statistically significant difference was seen between mean SUV obtained from ferumoxytol-enhanced and non-enhanced scans (mixed effects generalized linear model, $p > 0.05$).

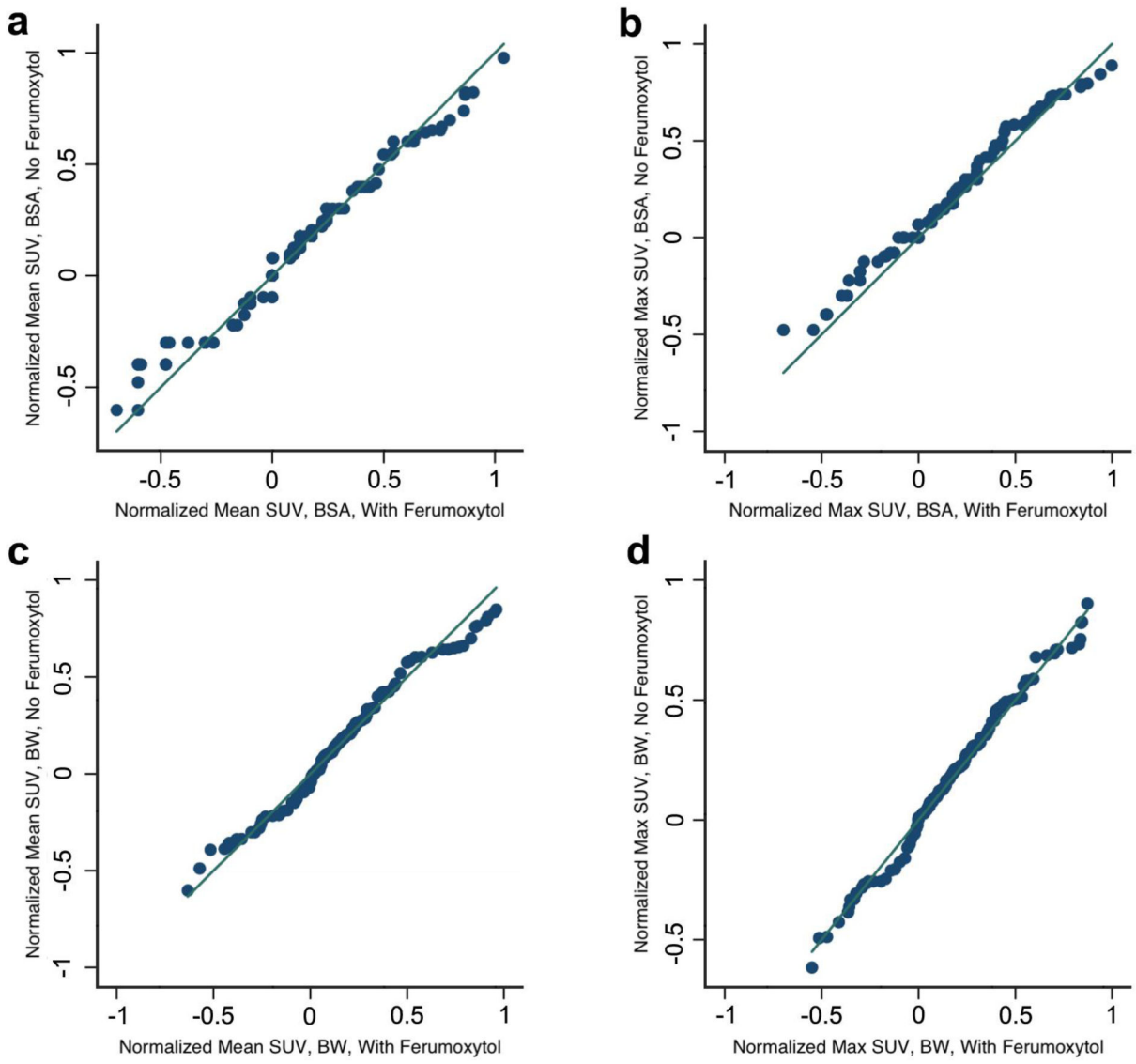

Figure 5.

Quantile-quantile plots for **a** mean SUV body surface area (bsa) and **b** $SUVmax_{bsa}$ and SUVmean body weight (bw) (**c**) and $SUVmax_{bw}$ (**d**) show equal distributions between both groups with Kolmogrov-Smirnov tests (all $p > 0.05$). Ferumoxytol patients were plotted on x-axis, and no-ferumoxytol patients were plotted on y-axis.